

# Pixel-Wise Contrastive Distillation

Junqiang Huang<sup>†‡</sup> Zichao Guo<sup>†</sup>  
Shopee

jq.huang.work@gmail.com zichao.guo@shopee.com

## Abstract

We present the first pixel-level self-supervised distillation framework specified for dense prediction tasks. Our approach, called Pixel-Wise Contrastive Distillation (PCD), distills knowledge by attracting the corresponding pixels from student’s and teacher’s output feature maps. This pixel-to-pixel distillation demands for maintaining the spatial information of teacher’s output. We propose a Spatial-Adaptor that adapts the well-trained projection/prediction head of the teacher used to encode vectorized features to processing 2D feature maps. SpatialAdaptor enables more informative pixel-level distillation, yielding a better student for dense prediction tasks. Besides, in light of the inadequate effective receptive fields of small models, we utilize a plug-in multi-head self-attention module to explicitly relate the pixels of student’s feature maps. Overall, our PCD outperforms previous self-supervised distillation methods on various dense prediction tasks. A backbone of ResNet-18 distilled by PCD achieves 37.4 AP<sup>bbbox</sup> and 34.0 AP<sup>mask</sup> with Mask R-CNN detector on COCO dataset, emerging as the first pre-training method surpassing the supervised pre-trained counterpart.

## 1. Introduction

Self-supervised learning (SSL) has emerged as a promising way for pre-training due to its remarkable progress for various computer vision tasks [6,9,21,23]. Without the need for annotations, self-supervised pre-trained models achieve similar or better transfer performance compared to the supervised counterparts. The advancement of SSL, however, appears to be limited to large models. Small models like ResNet-18 [25] show inferior results under the linear probing protocol as reported in [14,18,57]. Recently, the performance lag of small models has been effectively alleviated by self-supervised distillation [1,4,14,18,19,39,52,57,58,63], where teachers’ (large pre-trained models) knowledge

is transferred [2,5,28,48] to students (small models) in a self-supervised learning fashion.

The specific practice of self-supervised distillation methods can be summarized as the following two types: (i) minimizing the feature distance between students and teachers [1,4,18,19,52,57], (ii) classifying the semantic clusters generated by teachers [14,39,58,63]. These methods enable competitive performance of small models, especially on classification tasks (e.g., fine-grained and few-shot classification). But the improvement of dense prediction tasks like object detection and semantic segmentation is not so bright as that of classification tasks. This imbalanced status seemingly suggests that the favorable representations learned by teachers can only be *partially* transferred to students. A natural question to ask is: what hinders students from inheriting the knowledge beneficial to dense prediction tasks? In this study, we seek the answers to this question from the following aspects.

First, the distillation signals of current self-supervised distillation methods are mostly at image-level, while the rich *pixel-level knowledge* is yet to be utilized. These methods pursue a distilled student capable of extracting semantically separable features from images. But dense prediction tasks demand more—the pixels themselves should also be distinguishable. As opposed to large models, small models are hard to learn pixel-level knowledge from image-level supervision. Encouraging students to mimic teachers’ “vectorized” behaviors might fail to transfer the abundant pixel-level knowledge to small models. Driven by this, we present the first pixel-level self-supervised distillation framework, **Pixel-Wise Contrastive Distillation** (PCD), extending the idea of contrastive learning [22] by combining pixel-level knowledge distillation. For a given image, our PCD attracts the *corresponding* pixels from student’s and teacher’s output feature maps while separating student’s pixels and negative pixels of a memory queue [23]. In this manner, the student is spurred to mimic the teacher at pixel-level, resulting in more adequate knowledge transfer.

Second, it is not straightforward to distill pixel-level knowledge from the commonly adopted teachers pre-trained by image-level SSL methods [6,9,21,23]. These

<sup>†</sup>Equal Contribution  
<sup>‡</sup>corresponding author

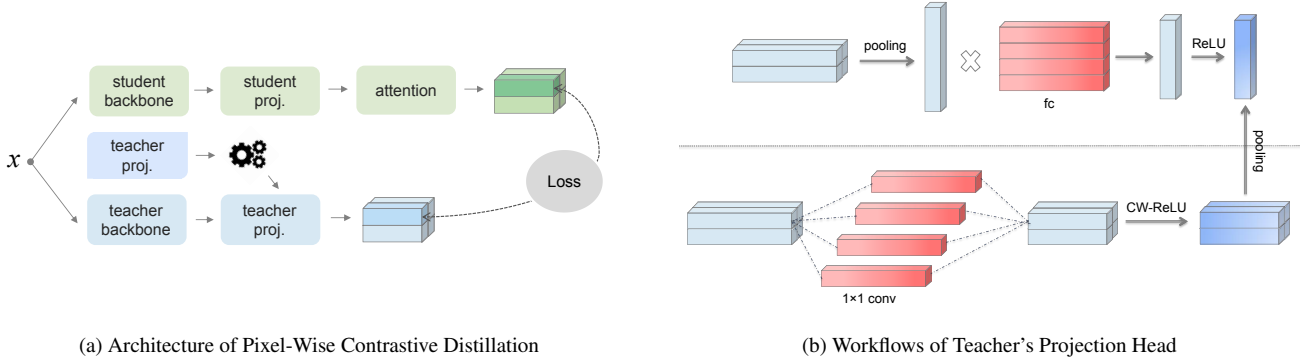



Figure 1. (a) is the specific architecture of Pixel-Wise Contrastive Distillation. Before distillation, the original teacher’s projection head is modified by SpatialAdaptor (represented by  in the figure). Distillation loss is the average contrastive loss computed over all corresponding pixel pairs of the student and the teacher. (b) depicts the workflows of teacher’s projection head before and after using SpatialAdaptor. The pooling layer on the far right is used for demonstrating the invariability of SpatialAdaptor. Best viewed in color.

teachers tend to project images into vectorized features, thus losing the spatial information *indispensable* to pixel-to-pixel distillation in our PCD. An intuitive practice to circumvent this issue would be to drop the well-trained projection/prediction head (a non-linear MLP attached to the backbone) and perform distillation before the global pooling layer. Nevertheless, we experimentally show the ineffectiveness of such simplistic approach, suggesting the projection/prediction head contains nonnegligible knowledge for pixel-level distillation. Towards the goal of leveraging this knowledge, we devise a *SpatialAdaptor* to adapt the projection/prediction head used to encode vectorized features to processing 2D feature maps while not changing the distribution of output features. Though conceptually simple, SpatialAdaptor is of great significance to pixel-level distillation.

Last, small models are innately weak in capturing spatial information from regions of large spans due to its limited capacity. We compare the effective receptive fields (ERF) [37] of a small model (ResNet-18) and a large model (ResNet-50) to verify this point. To overcome this natural deficiency, we insert a multi-head self-attention (MHSA) module [49] to the end of the student model, *explicitly* relating pixels within the output feature maps. Adding the MHSA module helps slightly enlarge the ERF of the small model, and consequently improves transferring results. The MHSA module only introduces a feasible cost of memory and computation during training and will be deprecated in fine-tuning. The concrete form of PCD is depicted in Fig. 1a.

We evaluate our PCD on several typical dense prediction tasks. Given the backbone of ResNet-18, PCD surpasses state-of-the-art results among all downstream tasks. The nontrivial advantages against competitive SSL methods designed for dense prediction tasks and previous image-level self-supervised distillation methods exhibit the supe-

riority of pixel-level supervision signal for self-supervised distillation. PCD achieves 37.4 AP<sup>bbbox</sup> and 34.0 AP<sup>mask</sup> on COCO dataset [34] by using Mask R-CNN detector [24] and ResNet-18-FPN [33] backbone, emerging as the first pre-training method outperforming the supervised pre-trained counterpart. Under the linear probing protocol, a ResNet-18 distilled by PCD obtains 65.1% top-1 accuracy on ImageNet.

Our PCD is robust to the choices of pre-trained teacher models and works well with various student backbone architectures. Students with larger backbones can compete with or even exceed the teacher on some dense prediction tasks. These results reveal an encouraging path for pre-training. We hope our findings will motivate future research.

## 2. Related Work

**Pixel/region-level self-supervised learning** aims to learn competitive representations specialized for dense prediction tasks. Following the philosophy of contrasting pixel/region-level features from different augmented views, these methods develop various *rules* to find the positive pairs.

Intuitive methods [40, 43, 54, 56, 59] record the offsets and the scaling factors induced by geometric transformations (*e.g.*, cropping, resizing, and flipping) to locate positive pairs of pixels/regions from different augmented views. In [3, 26], each pixel of the original image is classified into some appropriate categories by a heuristic method or some unsupervised semantic segmentation methods. Any two pixels or regions from the same category form a positive pair. SoCo [51] and ORL [55] utilize the selective search [47] to identify numerous regions containing a single object and perform region-level contrastive learning based on these regions. DenseCL [50] and Self-EMD [35] pair the pixels of feature maps from different views according to some certain rules, *e.g.*, minimizing the cosine distances

between pixels or finding the matching set with minimum earth mover’s distance [29].

Our PCD does not rely on sophisticated rules or preparations to pair pixels/regions. Instead, we *directly* contrast the feature maps projected by the student and the teacher from the same view of image, decoupling the requirement for delicate augmentation policies from the design of pre-training framework.

**Feature-based knowledge distillation** transfers knowledge by matching the *intermediate* features between a student and a teacher. Generally, these features are not comparable because of their different shapes, *i.e.*, number of channels and spatial size. It is a common practice to reshape the features of the student to have the same shape as the features of the teacher by a learnable module [44]. Some works [8, 27, 32, 61] transform both student’s and teacher’s features into tensors of same shape. In PCD, shape aligning (especially for the number of channels) is completed by student’s non-linear projection head. It is universally recognized that this projection head also improves the quality of learned representations in SSL [9, 10].

**Self-supervised distillation** transfers knowledge in a self-supervised learning fashion. CompRes [1] and SEED [18] propose to minimize feature similarity distribution between the student and the teacher. DoGo [4] and DisCo [19] add a distillation branch for easing the optimization problem of small models during self-supervised pre-training. Previous works [39, 58] train the student to classify the images based on the pseudo labels generated by teacher’s clustering. In BINGO [57], samples are grouped based on their similarity computed by the teacher, and the student learns to minimize intra-group distances. Recent work [14] simultaneously trains the teacher from scratch and perform distillation, where the student is guided by teacher’s on-the-fly clustering. Our PCD *differs* from these methods in that the distillation signal of the former is at pixel-level. Our goal is to pursue a student adept at dense prediction tasks.

### 3. Method

#### 3.1. Pixel-Wise Contrastive Distillation

Unlike general knowledge distillation methods in supervised learning, self-supervised distillation does not involve with labeled data. The supervision only comes from teachers, yielding a task-agnostic student that can be fine-tuned in various downstream tasks.

**Image-level self-supervised distillation.** Though varying dramatically in the specific rules of computing distillation loss, self-supervised knowledge distillation methods share one thing in common—the supervision signals are

all at *image-level*. Here, we describe a general formulation for these methods. An input image is fed to student’s and teacher’s backbone, generating feature maps,  $\mathbf{s} \in \mathbb{R}^{C_s \times H \times W}$  and  $\mathbf{t} \in \mathbb{R}^{C_t \times H \times W}$ , respectively.  $C$  is the number of channels.  $H$  and  $W$  are the spatial sizes. These feature maps are then global average/max pooled into vectorized features. The distillation loss  $\mathcal{L}$  with respect to a single input image is defined by:

$$\mathcal{L} = \mathcal{L}(\phi(\mathbf{s}), \phi(\mathbf{t})), \quad (1)$$

where  $\phi(\cdot)$  is the global pooling layer. Note that  $\mathcal{L}(\cdot, \cdot)$  is a function composition, but not a simple loss function like  $\ell_2$  distance. We let  $\phi$  be global average pooling for the ease of analysis, *i.e.*,  $\phi(\mathbf{x}) = \frac{1}{HW} \sum_i \mathbf{x}_i$ . Here  $i = (i_H, i_W)$  is a 2-tuple indexing the  $(i_H, i_W)$ -th pixel of feature maps.

Given the above unified formulation, we consider the derivative with respect to the  $i$ -th pixel of student’s feature maps  $\mathbf{s}_i$ . By chain rule, we have:

$$\frac{\partial \mathcal{L}}{\partial \mathbf{s}_i} = \frac{\partial \mathcal{L}}{\partial \phi} \frac{\partial \phi}{\partial \mathbf{s}_i} = \frac{1}{HW} \frac{\partial \mathcal{L}}{\partial \phi}. \quad (2)$$

It is obvious to see that  $\frac{\partial \mathcal{L}}{\partial \mathbf{s}_i}$  is a term *independent* from the position of the pixel. Teacher’s guidance is not detailed at pixel-level. There probably exists huge disparity between student’s and teacher’s pixel-level features. Consequently, it is far beyond reach for students (small models) to inherit competitive pixel-level knowledge possessed by teachers. We hypothesize that this may be the very reason of students’ imbalanced performance on classification and dense prediction tasks.

**Pixel-Wise Contrastive Distillation.** Motivated by the above analysis, we propose the first *pixel-level* self-supervised distillation framework, Pixel-Wise Contrastive Distillation (PCD). Our PCD transfers knowledge by attracting the positive pairs of pixels from students and teachers and repulsing the negative pairs.

Different from augmentation-invariant representation learning [9, 23, 38, 46, 50, 56], the positive pairs of PCD are from the *corresponding* pixels of student’s and teacher’s output feature maps for the same image, *i.e.*,  $(\mathbf{s}_i, \mathbf{t}_i)$ . Negative samples  $\{\mathbf{n}^k | k = 1, \dots, K\}$  are stored in a queue in conformity with MoCo [23]. For an input image, we optimize the average contrastive loss of all output pixels:

$$\mathcal{L}(\mathbf{s}, \mathbf{t}) = \frac{1}{HW} \sum_i \ell(\mathbf{s}_i, \mathbf{t}_i, \{\mathbf{n}^k\}), \quad (3)$$

---

It is reasonable to assume  $\mathbf{s}$  and  $\mathbf{t}$  have the same spatial size owing to the popular stage-wise designs of convolutional network architectures.

In CompRes [1], for example,  $\mathcal{L}$  is equivalent to first estimating the similarity distributions of the student and the teacher, then computing the KL divergence between distributions.

where  $\ell(\cdot, \cdot)$  stands for the contrastive loss function. We do not directly contrast  $\mathbf{s}_i$  and  $\mathbf{t}_i$  for they may have different dimensions (*i.e.*, the numbers of channels). Following SimCLR [9], we append a projection head  $\varphi(\cdot|\theta)$  (a non-linear MLP) to student’s backbone. The details of  $\varphi$  will be given in Sec. 3.2. The projection head  $\varphi$  serves as aligning  $\mathbf{s}_i$  and  $\mathbf{t}_i$  in terms of dimension. It will be removed once training is accomplished. We denote the projected output  $\varphi(\mathbf{s}_i|\theta)$  as  $\mathbf{s}_i^*$ . The concrete form of  $\ell$  is:

$$\ell = -\log \frac{\exp(\mathbf{s}_i^{*\top} \mathbf{t}_i / \tau)}{\exp(\mathbf{s}_i^{*\top} \mathbf{t}_i / \tau) + \sum_k \exp(\mathbf{s}_i^{*\top} \mathbf{n}^k / \tau)}, \quad (4)$$

where  $\tau$  is a temperature hyper-parameter. After back-propagation, teacher’s feature maps,  $\mathbf{t}$ , will be global pooled,  $\ell_2$ -normalized, and enqueued as a negative sample used for subsequent iterations. For notational convenience, we omit the  $\ell_2$ -normalization applied to  $\mathbf{s}_i^*$  and  $\mathbf{t}_i$ .

It is worth noting that  $\mathbf{s}$  and  $\mathbf{t}$  do not necessarily have the same spatial size. In the case of  $\mathbf{s}$  and  $\mathbf{t}$  having mismatched spatial size, we perform bilinear interpolation on  $\mathbf{t}$  to match the spatial size of  $\mathbf{s}$ . Further discussions are in Sec. 4.3.

**SpatialAdaptor.** For the models pre-trained by image-level SSL methods (*e.g.*, [6,9,21,23]), their projection/prediction heads (henceforth projection head for simplicity) are the stacked fully-connected (fc) layers with batch normalization (BN) layers and ReLU in between. They are used to project the global pooled features output by backbones. If adopting these models as teachers (a common practice in previous self-supervised distillation methods), one has to *remove* the global pooling layer and the projection heads to be compatible with our PCD. However, removing the well-trained projection heads will break the *integrity* of teachers. This in turn incurs knowledge loss, resulting in sub-optimal results for transfer learning. We will empirically verify this in Sec. 4.3.

To meet the demand of utilizing the fruitful knowledge of projection heads, we propose a *SpatialAdaptor* to adapting the projection heads to processing 2D inputs. We next discuss a simple case where the projection head only contains a fc layer ( $f$ ) and ReLU ( $\sigma$ ), to demonstrate how *SpatialAdaptor* works. Previously, the feature maps  $\mathbf{t}$  output by teacher’s backbone will be global pooled and fed to the projection head:

$$\begin{aligned} \sigma(f(\phi(\mathbf{t}))) &= \sigma\left(f\left(\frac{1}{HW} \sum_i \mathbf{t}_i\right)\right) \\ &= \sigma\left(\frac{1}{HW} \sum_i f(\mathbf{t}_i)\right). \end{aligned} \quad (5)$$

The second equality holds being a consequence of  $f$ ’s linearity. By interchanging  $f$  and  $\phi$ ,  $f$  now acts on pixels rather than vectorized features. It follows that  $f$  can be *reformulated* into a  $1 \times 1$  convolution (conv) layer with the stride of 1. This simple case does not consider the existence of any BN layer since fc and BN layers together can be fused into a linear function and represented by  $f$ .

Furthermore, we present the Channel-Wise ReLU (CW-ReLU) that masks out the channels whose mean are negative. Let  $\sigma^*$  denote CW-ReLU. By definition, we have:

$$\sigma(\phi(\mathbf{x})) = \phi(\sigma^*(\mathbf{x})). \quad (6)$$

This means the global pooling layer and the activation function are “*commutative*”. From Eq. (5) and the commutative property, we can interchange the global pooling layer and the activation function:

$$\sigma(f(\phi(\mathbf{t}))) = \phi(\sigma^*(f(\mathbf{t}))). \quad (7)$$

Note that  $\phi$  in the right-hand side of Eq. (7) is only used for illustrating the *invariability* of *SpatialAdaptor*. It will be omitted in actual use for maintaining spatial information.

We have shown how a projection head composed of a fc layer and ReLU is adapted by *SpatialAdaptor* to processing feature maps while not changing the feature distribution (Fig. 1b). As such, the integrity of teachers is maintained, and our PCD is made compatible with teachers pre-trained by various SSL methods. Though the case discussed above being so simple, *SpatialAdaptor* can easily apply to complex projection heads with more stacked fc layers and ReLU. *SpatialAdaptor* helps keep the integrity of teachers and makes our PCD compatible with teachers pre-trained by various SSL methods.

We are aware that the models pre-trained by pixel-level SSL methods [50,56] have projection heads processing 2D inputs. But this does *not* deprive the significance of *SpatialAdaptor*, because we do not want too much constraints on teacher’s pre-training methods. Such accessibility can also be seen as a strength of our PCD.

**Multi-head self-attention.** Apart from the granularity of distillation signals, the *intrinsic properties* (*e.g.*, limited capacity and smaller receptive field) of students also play a key role in the performance of dense prediction tasks. Consider the effective receptive field (ERF) [37] for an example. ERF measures how much each pixel contributes to the final prediction and has been proven to be closely related to the performance of abundant computer vision tasks [7,13]. Intuitively, models with larger ERF are able to capture information from a bigger area of image, leading to more robust and reliable predictions.

According to [37], we draw the ERFs of ResNet-50 and ResNet-18 [25] in Fig. 2. We can see a clear contrast



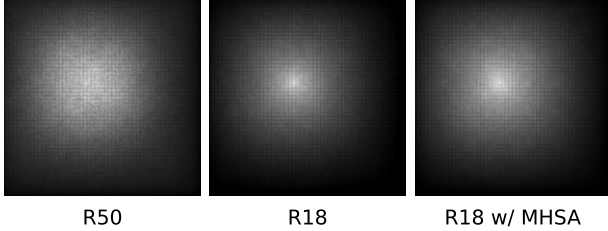


Figure 2. **Effective receptive field.** R50 and R18 are ResNet-50 and ResNet-18 respectively. R18 w/ MHSA stands for ResNet-18 enhanced by a multi-head self-attention module.

that ResNet-50 has larger ERF (larger bright region) than ResNet-18. Therefore, it is unrealistic to expect small models to perfectly capture rich spatial information like teachers without outside help.

The definition of ERF indicates allowing more pixels to participate in predictions helps enlarge ERF. From this perspective, we can enhance the student model by *explicitly* relating all pixels right before making predictions. This is made possible by a multi-head self-attention (MHSA) module [49]. Information from different pixels are aggregated together to make a more robust prediction. This module only induces a handful of memory and computation cost for training, and does not influence the fine-tuning phase. Equipped with the MHSA module, the ERF of ResNet-18 is slightly enlarged (shown in the third picture of Fig. 2).

### 3.2. Baseline Settings

In this section, we provide the necessary details for implementing our PCD.

**Teacher.** In most of our experiments, we adopt the ResNet-50 pre-trained by MoCo v3 [12] for 1000 epochs as the teacher. We use the momentum updated branch (*i.e.*, `momentum_encoder` of the checkpoint) of MoCo v3 model. The projection head has the following structure: FC–BN–ReLU–FC–BN. The last BN has no affine parameters. We drop it because its static normalization statistics slow down the convergence. The global pooling layer of the backbone is removed. Modified by SpatialAdaptor, the structure of the projection head becomes Conv–BN–CW–ReLU–Conv. The hidden and output dimension of the projection head is 4096 and 256 respectively. The shape of output feature maps is  $256 \times 7 \times 7$  (channels  $\times$  spatial size).

**Student.** By default, we use ResNet-18 as student’s backbone. It is followed by a projection head ( $\varphi$  mentioned above). We follow the asymmetric structure design in [11, 12, 21] and instantiate  $\varphi$  with two consecutive MLPs. The MLPs are structurally similar to teacher’s modified

The checkpoint can be found in <https://github.com/facebookresearch/moco-v3/blob/main/CONFIG.md>

projection head, except that the activation function is ReLU and that the input dimension of the first MLP is identical to the output dimension of student’s backbone. Next, we append a regular MHSA module [49] to the end of  $\varphi$ . The MHSA has 8 heads, each with an embedding dimension of 64. In each head, the feature maps are fed to three  $1 \times 1$  conv layers to produce queries, keys, and values, respectively. The attention values of all heads are concatenated and then projected by a  $1 \times 1$  conv layer to match with input features in dimension. The output of the MHSA module is used for computing the contrastive distillation loss.

**Distilling.** We perform self-supervised distillation on the ImageNet [45] training set. The image augmentation policy is the same as that proposed in [21], comprised of two distributions of augmentation. It generates a pair of augmented views for an input image. Our PCD computes distillation loss on each view and optimizes the mean of two losses. We observe this loss symmetrization brings about better convergence. We must point out that PCD with asymmetric loss also provides bright transfer performance (see in Sec. 4.2).

We use the LARS [60] optimizer to train for 100 epochs. The batch size is 1024. The base learning rate ( $lr$ ) is set to be 1.0 and scaled by the linear scaling rule [20]:  $lr \times \text{batch\_size} / 256$ . The learning rate is linearly increased to 4.0 for the first 10 epochs of training (warmup) and then decayed to 0 based on the cosine schedule. We use a weight decay of 0.00001 and a momentum of 0.9. All biases and the affine parameters of BN layers are excluded from the weight decay. We set the temperature of contrastive loss to be 0.2. The queue storing negative samples has a capacity of 65536.

## 4. Experiments

### 4.1. Evaluation Setup

Here, we provide some background for our fine-tuning experiments. We evaluate our PCD on VOC [17] object detection, COCO [34] object detection and instance segmentation, and CityScapes [15] semantic segmentation. The codebase for evaluation is Detectron2 [53]. We strictly follow the fine-tuning settings proposed in [23, 56] for fair comparisons. We also provide the linear probing accuracy on ImageNet.

It has been a notorious problem that fine-tuning LARS-trained models with optimization hyper-parameters best selected for SGD-trained counterparts yields sub-optimal performance [11, 31]. To address this, recent work [31] proposes NormRescale to scale the norm of LARS-trained weights by a specific anchor (*e.g.*, the norm of SGD-trained weights or a constant number). It helps the LARS-trained models fit to the optimization strategy of fine-tuning. When fine-tuning C4 or FCN backbones pre-trained by PCD, we

	ImageNet	VOC 07		VOC 07+12		COCO-C4		COCO-FPN		CityScapes
	Acc	AP <sub>50</sub>	AP	AP <sub>50</sub>	AP	AP <sup>bbox</sup>	AP <sup>mask</sup>	AP <sup>bbox</sup>	AP <sup>mask</sup>	IoU
Teacher	74.6	77.8	48.1	83.0	56.7	37.4	32.8	40.7	36.9	73.5
ImageNet Supervised	<b>69.8</b>	70.0	38.2	76.9	47.3	30.7	28.0	36.3	33.0	70.2
MoCo v2 [10]	48.7	69.7	40.2	77.5	49.7	30.7	27.9	35.0	31.8	70.4
PixPro [56]	41.4	71.5	42.3	78.5	51.1	30.9	28.1	35.8	32.6	70.3
CompRes [1]	63.9	71.3	41.2	78.4	50.4	31.4	28.4	35.7	32.4	70.3
DisCo [19]	63.5	62.5	30.7	72.6	40.1	28.2	25.8	36.0	32.8	69.3
BINGO [57]	64.2	70.4	39.9	77.8	49.3	31.1	28.2	36.2	32.8	71.0
PCD, asymmetric	64.2	72.7	42.7	79.3	51.5	31.9	28.8	37.0	33.7	71.6
PCD	65.1	<b>73.0</b>	<b>43.2</b>	<b>79.4</b>	<b>52.1</b>	<b>32.2</b>	<b>29.0</b>	<b>37.4</b>	<b>34.0</b>	<b>71.8</b>

Table 1. **Comparing different pre-trained models.** All pre-trained models adopt ResNet-18 as backbone. ImageNet supervised pre-trained model is from the model zoo of PyTorch [41]. Other pre-trained models are from our reproductions built on their officially released codes. For fair comparisons, we pre-trained these models for 100 epochs. We use the ResNet-50 pre-trained by MoCo v3 as teacher for all self-supervised distillation methods. The best results are marked in **bold**, and the second best are marked in *gray* (exclusive of the teacher).

employ this technique to multiply the weights by a constant 0.25. Multiplying a constant is an efficient choice for not introducing extra training cost.

**VOC object detection.** We use a C4 backbone with Faster R-CNN [42] detector. We evaluate the pre-trained models under two fine-tuning settings. The first is to train on `trainval2007` set for 9k iterations, and the second is to train on `trainval07+12` set for 24k iterations. We use the same fine-tuning settings as per [23]. Fine-tuned models are evaluated on `test2007` set. For better reproducibility, we report the average AP<sub>50</sub> and AP over 5 runs.

**COCO object detection and instance segmentation.** We use two types of backbone, C4 and FPN, for fine-tuning on COCO dataset. The detector is Mask R-CNN [24]. Pre-trained models are fine-tuned on `train2017` set according to the  $1\times$  optimization setting (about 12 COCO epochs). We report AP<sup>bbox</sup> for object detection and AP<sup>mask</sup> for instance segmentation on `val2017` set.

**CityScapes semantic segmentation.** We implement a FCN-like [36] structure based on pre-trained backbones. A newly initialized BN layer is added to the end of pre-trained backbones for helping optimization. Subsequently, we append two atrous convolutional blocks, each with a  $3\times 3$  conv layer of 256 output channels, a BN layer, and ReLU. The conv layers have stride 1, dilation 6, and padding 6. The prediction layer is a  $1\times 1$  conv layer with 19 output channels (19 classes), whose outputs are then bilinearly interpolated to match the size of input images. Fine-tuning takes 90k iterations on `train.fine` set. More detailed information of fine-tuning can be found in Appendix. We report the average IoU on `val` set over 5 runs.

**Linear probing in ImageNet.** We freeze the backbones pre-trained by PCD and train a linear classifier on the ImageNet training set. We use nesterov SGD to train for 100 epochs. The batch size is 1024, and the learning rate is 0.8 (base  $lr = 0.2$ ). We decay the learning rate to 0 according to the cosine schedule without restart. The momentum is 0.9, and the weight decay is 0. We use a vanilla image augmentation policy containing random cropping, resizing to  $224\times 224$ , and horizontal flipping. We report the single-crop classification accuracy on the ImageNet validation set.

## 4.2. Main Results

In Tab. 1, we compare our PCD to the following competitive pre-training methods, supervised pre-training, SSL methods, and self-supervised distillation methods. Our PCD shows impressive generalization capacity: it outperforms all competitors on dense prediction tasks. We achieves 37.4 AP<sup>bbox</sup> and 34.0 AP<sup>mask</sup> on COCO using Mask R-CNN detector and ResNet-18-FPN backbone, emerging as the first pre-training method surpassing the supervised pre-trained model on this benchmark. Under the linear probing protocol, our PCD also achieves decent top-1 accuracy (65.1%), which makes PCD a well-rounded self-supervised distillation method.

We notice that some competitors (*e.g.*, supervised learning, MoCo v2 [10], and CompRes [1]) are pre-trained by asymmetric loss. Here, we provide a asymmetric variant of PCD to exclude the effect of loss symmetrization. The change is simple: we adopt the symmetric augmentation policy as per [21], and sample one augmented view from each input image during training. Indeed, the symmetric loss endows PCD with better performance, but asymmet-

	VOC 07+12		COCO-FPN		CityScapes
	AP <sub>50</sub>	AP	AP <sup>bbox</sup>	AP <sup>mask</sup>	IoU
image-level	78.7	49.8	36.5	33.3	71.1
pixel-level	<b>79.4</b>	<b>52.1</b>	<b>37.4</b>	<b>34.0</b>	<b>71.8</b>

Table 2. **Pixel-level vs. image-level.** We compare PCD to image-level contrastive distillation. The backbone is ResNet-18 and pre-trained for 100 epochs. The best results are marked in **bold**.

	VOC 07+12		COCO-FPN		CityScapes
	AP <sub>50</sub>	AP	AP <sup>bbox</sup>	AP <sup>mask</sup>	IoU
(a)	76.0	48.8	36.5	33.2	70.1
(b)	77.9	50.6	36.8	33.6	70.7
(c)	77.3	50.1	36.3	33.1	69.6
(d)	77.8	50.7	36.6	33.2	70.1
ours	<b>79.4</b>	<b>52.1</b>	<b>37.4</b>	<b>34.0</b>	<b>71.8</b>

Table 3. **Ablations on SpatialAdaptor.** We compare four variants of PCD (a-d) to examine the necessity of SpatialAdaptor. The backbone is ResNet-18 and pre-trained for 100 epochs. The best results are marked in **bold**.

ric variant still achieves the second best results on all tasks (marked as gray in Tab. 1). PCD’s *nontrivial* advantages against other self-supervised distillation methods have confirmed the fact that *pixel-level* distillation signals are the key to transferring knowledge conducive to dense prediction tasks.

### 4.3. Ablation Experiments

We perform extensive ablation experiments to analyze PCD. Unless specified, we adopt the training settings mentioned in Sec. 3.2.

**Pixel-level vs. image-level.** To directly compare pixel-level and image-level distillation, we develop an image-level variant of PCD. This variant vectorizes student’s and teacher’s output feature maps by an extra global average pooling layer and computes contrastive loss on these vectorized features. It has highly competitive results (Tab. 2) like those image-level self-supervised distillation methods in Tab. 1, revealing the effectiveness of contrastive loss used for self-supervised distillation. But it still *lags behind* the original PCD on all downstream tasks. This gap further confirms the importance of pixel-level distillation signal.

**Ablation on SpatialAdaptor.** We examine the necessity of SpatialAdaptor for learning competitive representations. Without resorting to SpatialAdaptor, we remove teacher’s projection head (along with the global pooling layer) and simply use the feature maps output by teacher’s backbone for computing contrastive loss (variant (a)). The evaluation metrics AP<sub>50</sub> and AP on VOC are rather low (Tab. 3

	VOC 07+12		COCO-FPN		CityScapes
	AP <sub>50</sub>	AP	AP <sup>bbox</sup>	AP <sup>mask</sup>	IoU
w/o MHSA	79.2	51.8	37.1	33.7	71.6
extra pred.	79.1	52.0	37.2	33.7	71.2
ours	<b>79.4</b>	<b>52.1</b>	<b>37.4</b>	<b>34.0</b>	<b>71.8</b>

Table 4. **Ablations on MHSA.** We ablate the design of MHSA. “extra pred.” stands for replacing the MHSA module by an extra prediction head. The backbone is ResNet-18 and pre-trained for 100 epochs. The best results are marked in **bold**.

(a)). This variant overlooks the fact that teacher’s feature maps have numerous zeros post-processing by ReLU while student’s do not. Contrasting two features from different distributions naturally leads to sub-optimal results.

For more reasonable comparisons, we introduce two more variants extended from variant (a). Variant (b) adds ReLU after the MHSA module. Variant (c) removes the MHSA module and adds ReLU after student’s projection head. Overall, these two variants (Tab. 3 (b-c)) are still significantly worse than PCD. And they are no better than the image-level self-supervised distillation methods in Tab. 1 and Tab. 2. We argue that preserving the integrity of teachers (with the help of SpatialAdaptor) is of vital importance to pixel-level distillation. Otherwise, it will notably lower the quality of learned representations.

Additionally, we study the impact of invariability of SpatialAdaptor by replacing CW-ReLU with ReLU (variant (d)). We observe that keeping the distribution of teacher’s learned features unchanged has massive gains on dense prediction tasks (Tab. 3 (d)). In sum, SpatialAdaptor is an essential component of PCD, enabling more *informative* pixel-wise distillation from teachers pre-trained by image-level SSL methods.

**Ablation on multi-head self-attention.** The MHSA module of PCD aims to explicitly relate pixels. We ablate this design in Tab. 4. Although removing the MHSA module meets slight performance drop, it can still be regarded as a competitive framework for self-supervised distillation. Another plausible explanation for the positive impact of the MHSA module is that it works like a prediction head to promote the quality of learned representations [11, 12, 21]. We thus supersede the MHSA module by an extra prediction head of roughly the same parameters like the MHSA module. This design does not bring any improvement (Tab. 4), suggesting that explicitly relating pixels is useful for PCD.

**Different teachers.** Both MoCo v3 and PCD are trained with contrastive loss. To exclude the positive or negative effect induced by optimizing the same type of loss, we consider using teachers pre-trained by SwAV [6], BYOL [21],

backbone	pre-training method	VOC 07		VOC 07+12		COCO-C4		COCO-FPN		CityScapes
		AP <sub>50</sub>	AP	AP <sub>50</sub>	AP	AP <sup>bbox</sup>	AP <sup>mask</sup>	AP <sup>bbox</sup>	AP <sup>mask</sup>	IoU
ResNet-50	SwAV	72.1	41.7	79.0	51.2	31.9	28.8	37.1	33.7	70.7
ResNet-50	BYOL	71.7	42.6	78.9	51.5	32.0	29.0	37.0	33.7	71.0
ResNet-50	Barlow Twins	70.7	41.6	78.4	50.7	31.3	28.4	35.9	32.7	70.9
ViT-Base	MoCo v3	70.6	41.7	78.1	51.1	31.3	28.5	36.6	33.6	71.4

Table 5. **Fine-tuning results of PCD with different teachers.** The student backbone is ResNet-18. All teacher models are from the officially released checkpoints. We refer to Appendix for more details about these teachers.

	pre-training method	VOC 07		VOC 07+12		COCO-C4		COCO-FPN		CityScapes
		AP <sub>50</sub>	AP	AP <sub>50</sub>	AP	AP <sup>bbox</sup>	AP <sup>mask</sup>	AP <sup>bbox</sup>	AP <sup>mask</sup>	IoU
ResNet-34	supervised	74.8	45.0	81.0	55.0	37.7	32.9	39.4	35.6	71.9
	PCD	<b>76.3</b>	<b>49.1</b>	<b>82.0</b>	<b>58.2</b>	<b>38.2</b>	<b>33.7</b>	<b>40.9</b>	<b>37.0</b>	<b>73.2</b>
ResNet-50	supervised	75.2	44.5	81.5	54.1	38.2	33.5	40.2	36.3	72.3
	PCD	<b>77.0</b>	<b>49.0</b>	<b>82.8</b>	<b>57.7</b>	<b>40.1</b>	<b>34.9</b>	<b>42.4</b>	<b>38.1</b>	<b>73.3</b>
MobileNet v3	supervised	67.9	36.7	76.2	46.4	30.6	27.9	35.8	32.7	68.3
	PCD	<b>73.9</b>	<b>40.8</b>	<b>79.3</b>	<b>49.9</b>	<b>32.8</b>	<b>29.6</b>	<b>37.7</b>	<b>34.3</b>	<b>69.0</b>

Table 6. **Fine-tuning results of PCD with different student backbones.** The teacher used for PCD is ResNet-50 pre-trained by MoCo v3. The student backbones are ResNet-18, ResNet-34, ResNet-50, and MobileNet v3 (Large). We also fine-tune the supervised pre-trained counterparts for contrast. We refer to Appendix for more implementation details. The best results for each backbone are marked as **bold**.

and Barlow Twins [62]. The fine-tuning results of Tab. 5 show that these teachers can also inspire favorable representations. It can be concluded that PCD is *robust* to the choices of teacher models.

Beyond typical convolutional architectures, we try using ViT [16] as the teacher to study the effect of cross-architectures distillation. There is an innate obstacle for ResNet-18 to imitate ViT at pixel-level, since they differ in the resolutions of output feature maps. Therefore, we downsample ViT’s output by a  $2 \times 2$  average pooling layer with a stride of 2. It leads to acceptable results on dense prediction tasks, whereas unsatisfying linear top-1 accuracy (57.6%) on ImageNet. We believe cross-architectures distillation (between CNNs and transformers) is a noteworthy problem for future research.

**Different students.** We investigate the effectiveness of PCD on different student backbones: ResNet-34, ResNet-50, and MobileNet v3 (Large) [30]. Compared to supervised pre-training, our PCD consistently outperforms on all backbones (Tab. 6). A clear *trend* is that backbones with larger capacity (from ResNet-18 to ResNet-50) have better transfer performance. A distilled ResNet-34 or ResNet-50 can rival or even beat the teacher (referred to Tab. 1) on some downstream tasks, marking the practicability of our PCD.

ViT-Base has  $14 \times 14$  output patches for  $224 \times 224$  input, and we treat each patch as a pixel.

## 5. Conclusion

Self-supervised pre-training has shown its great potential for many computer vision tasks. But its remarkable progress seems to be bound together with large models. Practitioners find it struggling to apply SSL methods on small models. Considering the necessity of small models for edge devices or resource constraint regime, it is much essential to tackle this problem. Recently, self-supervised knowledge distillation methods have been proposed to effectively boost the accuracy of small models on classification tasks.

We study another equally important yet unexplored problem: how to promote the transfer performance of small models on dense prediction tasks. From our extensive experiments, we find it difficult for small models to learn pixel-level knowledge from image-level pretext tasks, even with distillation signals. Such observation is in contrast to the case of large models: ResNet-50 pre-trained by MoCo v2 shows competitiveness on VOC and COCO object detection. This can be interpreted as the inefficiency of small models to implicitly learn from image-level pretext tasks. We therefore are inspired to propose the first pixel-level self-supervised distillation framework, enabling distilling a more competitive student on dense prediction tasks. We hope our observations and experiments can motivate future research.



## References

- [1] Soroush Abbasi Koohpayegani, Ajinkya Tejankar, and Hamed Pirsiavash. Compress: Self-supervised learning by compressing representations. *Advances in Neural Information Processing Systems*, 33:12980–12992, 2020.
- [2] Jimmy Ba and Rich Caruana. Do deep nets really need to be deep? *Advances in neural information processing systems*, 27, 2014.
- [3] Yutong Bai, Xinlei Chen, Alexander Kirillov, Alan Yuille, and Alexander C Berg. Point-level region contrast for object detection pre-training. In *Proceedings of the IEEE/CVF Conference on Computer Vision and Pattern Recognition*, pages 16061–16070, 2022.
- [4] Prashant Bhat, Elahe Arani, and Bahram Zonooz. Distill on the go: Online knowledge distillation in self-supervised learning. In *Proceedings of the IEEE/CVF Conference on Computer Vision and Pattern Recognition*, pages 2678–2687, 2021.
- [5] Cristian Bucilua, Rich Caruana, and Alexandru Niculescu-Mizil. Model compression. In *Proceedings of the 12th ACM SIGKDD international conference on Knowledge discovery and data mining*, pages 535–541, 2006.
- [6] Mathilde Caron, Ishan Misra, Julien Mairal, Priya Goyal, Piotr Bojanowski, and Armand Joulin. Unsupervised learning of visual features by contrasting cluster assignments. *Advances in Neural Information Processing Systems*, 33:9912–9924, 2020.
- [7] Liang-Chieh Chen, George Papandreou, Florian Schroff, and Hartwig Adam. Rethinking atrous convolution for semantic image segmentation. *arXiv preprint arXiv:1706.05587*, 2017.
- [8] Pengguang Chen, Shu Liu, Hengshuang Zhao, and Jiaya Jia. Distilling knowledge via knowledge review. In *Proceedings of the IEEE/CVF Conference on Computer Vision and Pattern Recognition*, pages 5008–5017, 2021.
- [9] Ting Chen, Simon Kornblith, Mohammad Norouzi, and Geoffrey Hinton. A simple framework for contrastive learning of visual representations. In *International conference on machine learning*, pages 1597–1607. PMLR, 2020.
- [10] Xinlei Chen, Haoqi Fan, Ross Girshick, and Kaiming He. Improved baselines with momentum contrastive learning. *arXiv preprint arXiv:2003.04297*, 2020.
- [11] Xinlei Chen and Kaiming He. Exploring simple siamese representation learning. In *Proceedings of the IEEE/CVF Conference on Computer Vision and Pattern Recognition*, pages 15750–15758, 2021.
- [12] Xinlei Chen, Saining Xie, and Kaiming He. An empirical study of training self-supervised vision transformers. In *Proceedings of the IEEE/CVF International Conference on Computer Vision*, pages 9640–9649, 2021.
- [13] Yunpeng Chen, Haoqi Fan, Bing Xu, Zhicheng Yan, Yan-nis Kalantidis, Marcus Rohrbach, Shuicheng Yan, and Jiashi Feng. Drop an octave: Reducing spatial redundancy in convolutional neural networks with octave convolution. In *Proceedings of the IEEE/CVF International Conference on Computer Vision*, pages 3435–3444, 2019.
- [14] Hee Min Choi, Hyoa Kang, and Dokwan Oh. Unsupervised representation transfer for small networks: I believe i can distill on-the-fly. *Advances in Neural Information Processing Systems*, 34:24645–24658, 2021.
- [15] Marius Cordts, Mohamed Omran, Sebastian Ramos, Timo Rehfeld, Markus Enzweiler, Rodrigo Benenson, Uwe Franke, Stefan Roth, and Bernt Schiele. The cityscapes dataset for semantic urban scene understanding. In *Proceedings of the IEEE conference on computer vision and pattern recognition*, pages 3213–3223, 2016.
- [16] Alexey Dosovitskiy, Lucas Beyer, Alexander Kolesnikov, Dirk Weissenborn, Xiaohua Zhai, Thomas Unterthiner, Mostafa Dehghani, Matthias Minderer, Georg Heigold, Sylvain Gelly, et al. An image is worth 16x16 words: Transformers for image recognition at scale. *arXiv preprint arXiv:2010.11929*, 2020.
- [17] Mark Everingham, SM Eslami, Luc Van Gool, Christopher KI Williams, John Winn, and Andrew Zisserman. The pascal visual object classes challenge: A retrospective. *International journal of computer vision*, 111(1):98–136, 2015.
- [18] Zhiyuan Fang, Jianfeng Wang, Lijuan Wang, Lei Zhang, Yezhou Yang, and Zicheng Liu. Seed: Self-supervised distillation for visual representation. *arXiv preprint arXiv:2101.04731*, 2021.
- [19] Yuting Gao, Jia-Xin Zhuang, Ke Li, Hao Cheng, Xiaowei Guo, Feiyue Huang, Rongrong Ji, and Xing Sun. Disco: Remedy self-supervised learning on lightweight models with distilled contrastive learning. *arXiv preprint arXiv:2104.09124*, 2021.
- [20] Priya Goyal, Piotr Dollár, Ross Girshick, Pieter Noordhuis, Lukasz Wesolowski, Aapo Kyrola, Andrew Tulloch, Yangqing Jia, and Kaiming He. Accurate, large mini-batch sgd: Training imagenet in 1 hour. *arXiv preprint arXiv:1706.02677*, 2017.
- [21] Jean-Bastien Grill, Florian Strub, Florent Altché, Corentin Tallec, Pierre Richemond, Elena Buchatskaya, Carl Doersch, Bernardo Avila Pires, Zhaohan Guo, Mohammad Gheshlaghi Azar, et al. Bootstrap your own latent—a new approach to self-supervised learning. *Advances in neural information processing systems*, 33:21271–21284, 2020.
- [22] Raia Hadsell, Sumit Chopra, and Yann LeCun. Dimensionality reduction by learning an invariant mapping. In *2006 IEEE Computer Society Conference on Computer Vision and Pattern Recognition (CVPR'06)*, volume 2, pages 1735–1742. IEEE, 2006.
- [23] Kaiming He, Haoqi Fan, Yuxin Wu, Saining Xie, and Ross Girshick. Momentum contrast for unsupervised visual representation learning. In *Proceedings of the IEEE/CVF conference on computer vision and pattern recognition*, pages 9729–9738, 2020.
- [24] Kaiming He, Georgia Gkioxari, Piotr Dollár, and Ross Girshick. Mask r-cnn. In *Proceedings of the IEEE international conference on computer vision*, pages 2961–2969, 2017.
- [25] Kaiming He, Xiangyu Zhang, Shaoqing Ren, and Jian Sun. Deep residual learning for image recognition. In *Proceedings of the IEEE conference on computer vision and pattern recognition*, pages 770–778, 2016.

- [26] Olivier J Hénaff, Skanda Koppula, Jean-Baptiste Alayrac, Aaron Van den Oord, Oriol Vinyals, and João Carreira. Efficient visual pretraining with contrastive detection. In *Proceedings of the IEEE/CVF International Conference on Computer Vision*, pages 10086–10096, 2021.
- [27] Byeongho Heo, Jeesoo Kim, Sangdoon Yun, Hyojin Park, Nojun Kwak, and Jin Young Choi. A comprehensive overhaul of feature distillation. In *Proceedings of the IEEE/CVF International Conference on Computer Vision*, pages 1921–1930, 2019.
- [28] Geoffrey Hinton, Oriol Vinyals, Jeff Dean, et al. Distilling the knowledge in a neural network. *arXiv preprint arXiv:1503.02531*, 2(7), 2015.
- [29] Frank L Hitchcock. The distribution of a product from several sources to numerous localities. *Journal of mathematics and physics*, 20(1-4):224–230, 1941.
- [30] Andrew Howard, Mark Sandler, Grace Chu, Liang-Chieh Chen, Bo Chen, Mingxing Tan, Weijun Wang, Yukun Zhu, Ruoming Pang, Vijay Vasudevan, et al. Searching for mobilenetv3. In *Proceedings of the IEEE/CVF international conference on computer vision*, pages 1314–1324, 2019.
- [31] Junqiang Huang, Xiangwen Kong, and Xiangyu Zhang. Revisiting the critical factors of augmentation-invariant representation learning. In *European Conference on Computer Vision*, pages 42–58. Springer, 2022.
- [32] Jangho Kim, SeongUk Park, and Nojun Kwak. Paraphrasing complex network: Network compression via factor transfer. *Advances in neural information processing systems*, 31, 2018.
- [33] Tsung-Yi Lin, Piotr Dollár, Ross Girshick, Kaiming He, Bharath Hariharan, and Serge Belongie. Feature pyramid networks for object detection. In *Proceedings of the IEEE conference on computer vision and pattern recognition*, pages 2117–2125, 2017.
- [34] Tsung-Yi Lin, Michael Maire, Serge Belongie, James Hays, Pietro Perona, Deva Ramanan, Piotr Dollár, and C Lawrence Zitnick. Microsoft coco: Common objects in context. In *European conference on computer vision*, pages 740–755. Springer, 2014.
- [35] Songtao Liu, Zeming Li, and Jian Sun. Self-emd: Self-supervised object detection without imagenet. *arXiv preprint arXiv:2011.13677*, 2020.
- [36] Jonathan Long, Evan Shelhamer, and Trevor Darrell. Fully convolutional networks for semantic segmentation. In *Proceedings of the IEEE conference on computer vision and pattern recognition*, pages 3431–3440, 2015.
- [37] Wenjie Luo, Yujia Li, Raquel Urtasun, and Richard Zemel. Understanding the effective receptive field in deep convolutional neural networks. *Advances in neural information processing systems*, 29, 2016.
- [38] Ishan Misra and Laurens van der Maaten. Self-supervised learning of pretext-invariant representations. In *Proceedings of the IEEE/CVF Conference on Computer Vision and Pattern Recognition*, pages 6707–6717, 2020.
- [39] Mehdi Noroozi, Ananth Vinjimoor, Paolo Favaro, and Hamed Pirsiavash. Boosting self-supervised learning via knowledge transfer. In *Proceedings of the IEEE conference on computer vision and pattern recognition*, pages 9359–9367, 2018.
- [40] Pedro O O Pinheiro, Amjad Almahairi, Ryan Benmalek, Florian Golemo, and Aaron C Courville. Unsupervised learning of dense visual representations. *Advances in Neural Information Processing Systems*, 33:4489–4500, 2020.
- [41] Adam Paszke, Sam Gross, Francisco Massa, Adam Lerer, James Bradbury, Gregory Chanan, Trevor Killeen, Zeming Lin, Natalia Gimelshein, Luca Antiga, Alban Desmaison, Andreas Kopf, Edward Yang, Zachary DeVito, Martin Raison, Alykhan Tejani, Sasank Chilamkurthy, Benoit Steiner, Lu Fang, Junjie Bai, and Soumith Chintala. Pytorch: An imperative style, high-performance deep learning library. In H. Wallach, H. Larochelle, A. Beygelzimer, F. d’Alché-Buc, E. Fox, and R. Garnett, editors, *Advances in Neural Information Processing Systems 32*, pages 8024–8035. Curran Associates, Inc., 2019.
- [42] Shaoqing Ren, Kaiming He, Ross Girshick, and Jian Sun. Faster r-cnn: Towards real-time object detection with region proposal networks. *Advances in neural information processing systems*, 28, 2015.
- [43] Byungseok Roh, Wuhyun Shin, Ildoo Kim, and Sungwoong Kim. Spatially consistent representation learning. In *Proceedings of the IEEE/CVF Conference on Computer Vision and Pattern Recognition*, pages 1144–1153, 2021.
- [44] Adriana Romero, Nicolas Ballas, Samira Ebrahimi Kahou, Antoine Chassang, Carlo Gatta, and Yoshua Bengio. Fitnets: Hints for thin deep nets. *arXiv preprint arXiv:1412.6550*, 2014.
- [45] Olga Russakovsky, Jia Deng, Hao Su, Jonathan Krause, Sanjeev Satheesh, Sean Ma, Zhiheng Huang, Andrej Karpathy, Aditya Khosla, Michael Bernstein, et al. Imagenet large scale visual recognition challenge. *International journal of computer vision*, 115(3):211–252, 2015.
- [46] Yonglong Tian, Dilip Krishnan, and Phillip Isola. Contrastive multiview coding. In *European conference on computer vision*, pages 776–794. Springer, 2020.
- [47] Jasper RR Uijlings, Koen EA Van De Sande, Theo Gevers, and Arnold WM Smeulders. Selective search for object recognition. *International journal of computer vision*, 104(2):154–171, 2013.
- [48] Ruth Urner, Shai Shalev-Shwartz, and Shai Ben-David. Access to unlabeled data can speed up prediction time. In *ICML*, 2011.
- [49] Ashish Vaswani, Noam Shazeer, Niki Parmar, Jakob Uszkoreit, Llion Jones, Aidan N Gomez, Łukasz Kaiser, and Illia Polosukhin. Attention is all you need. *Advances in neural information processing systems*, 30, 2017.
- [50] Xinlong Wang, Rufeng Zhang, Chunhua Shen, Tao Kong, and Lei Li. Dense contrastive learning for self-supervised visual pre-training. In *Proceedings of the IEEE/CVF Conference on Computer Vision and Pattern Recognition*, pages 3024–3033, 2021.
- [51] Fangyun Wei, Yue Gao, Zhirong Wu, Han Hu, and Stephen Lin. Aligning pretraining for detection via object-level contrastive learning. *Advances in Neural Information Processing Systems*, 34:22682–22694, 2021.

- [52] Kan Wu, Jinnian Zhang, Houwen Peng, Mengchen Liu, Bin Xiao, Jianlong Fu, and Lu Yuan. Tinyvit: Fast pretraining distillation for small vision transformers. *arXiv preprint arXiv:2207.10666*, 2022.
- [53] Yuxin Wu, Alexander Kirillov, Francisco Massa, Wan-Yen Lo, and Ross Girshick. Detectron2. <https://github.com/facebookresearch/detectron2>, 2019.
- [54] Tete Xiao, Colorado J Reed, Xiaolong Wang, Kurt Keutzer, and Trevor Darrell. Region similarity representation learning. In *Proceedings of the IEEE/CVF International Conference on Computer Vision*, pages 10539–10548, 2021.
- [55] Jiahao Xie, Xiaohang Zhan, Ziwei Liu, Yew Soon Ong, and Chen Change Loy. Unsupervised object-level representation learning from scene images. *Advances in Neural Information Processing Systems*, 34:28864–28876, 2021.
- [56] Zhenda Xie, Yutong Lin, Zheng Zhang, Yue Cao, Stephen Lin, and Han Hu. Propagate yourself: Exploring pixel-level consistency for unsupervised visual representation learning. In *Proceedings of the IEEE/CVF Conference on Computer Vision and Pattern Recognition*, pages 16684–16693, 2021.
- [57] Haohang Xu, Jiemin Fang, Xiaopeng Zhang, Lingxi Xie, Xinggang Wang, Wenrui Dai, Hongkai Xiong, and Qi Tian. Bag of instances aggregation boosts self-supervised distillation. In *International Conference on Learning Representations*, 2021.
- [58] Xueting Yan, Ishan Misra, Abhinav Gupta, Deepti Ghadiyaram, and Dhruv Mahajan. Clusterfit: Improving generalization of visual representations. In *Proceedings of the IEEE/CVF Conference on Computer Vision and Pattern Recognition*, pages 6509–6518, 2020.
- [59] Ceyuan Yang, Zhirong Wu, Bolei Zhou, and Stephen Lin. Instance localization for self-supervised detection pretraining. In *Proceedings of the IEEE/CVF Conference on Computer Vision and Pattern Recognition*, pages 3987–3996, 2021.
- [60] Yang You, Igor Gitman, and Boris Ginsburg. Large batch training of convolutional networks. *arXiv preprint arXiv:1708.03888*, 2017.
- [61] Sergey Zagoruyko and Nikos Komodakis. Paying more attention to attention: Improving the performance of convolutional neural networks via attention transfer. *arXiv preprint arXiv:1612.03928*, 2016.
- [62] Jure Zbontar, Li Jing, Ishan Misra, Yann LeCun, and Stéphane Deny. Barlow twins: Self-supervised learning via redundancy reduction. In *International Conference on Machine Learning*, pages 12310–12320. PMLR, 2021.
- [63] Kai Zheng, Yuanjiang Wang, and Ye Yuan. Boosting contrastive learning with relation knowledge distillation. In *Proceedings of the AAAI Conference on Artificial Intelligence*, volume 36, pages 3508–3516, 2022.

## A. Details of Fine-Tuning Experiments

### A.1. Fine-Tuning on CityScapes

The fine-tuning hyper-parameters are listed as follows:

Configuration	Value
optimizer	SGD
base learning rate	0.01
momentum	0.9
weight decay	1e-4
batch size	16
training steps	90000
learning rate schedule	WarmupMultiStepLR
warmup iters	1000
decay milestones	63000, 81000
shortest edge of resizing	[512, 768, ..., 2048]
max input size	4096
random cropping	True
random flipping	True

### A.2. Fine-Tuning MobileNet v3 (Large)

MobileNet v3 (Large) [30] is not a stage-wise architecture like ResNet series [25]. We have to manually define the “stem” and “res” stages in MobileNet v3 (Large) to fit in Detectron2. The rules for partitioning the modules of MobileNet v3 (Large) are: i) modules with the same stride belong to the same partition; ii) res4 must be of stride 16. We show the partitioning results:

index	modules	total stride	partitions
1	conv	2	stem
2	IBN	2	
3	IBN	4	res2
4	IBN	4	
5	IBN	8	res3
6	IBN	8	
7	IBN	8	
8	IBN	16	res4
9	IBN	16	
10	IBN	16	
11	IBN	16	
12	IBN	16	
13	IBN	16	
14	IBN	32	res5
15	IBN	32	
16	IBN	32	
17	conv	32	

### A.3. Distilling from Different Teachers

In Tab. 5, we try using other models as teachers. Most of checkpoints are from the official repository, except for BYOL [21]. The ResNet-50 [25] pre-trained by BYOL are from the implementation of [31]. We list out the URLs for downloading these models:

- MoCo v3 (ResNet-50) [12]: <https://dl.fbaipublicfiles.com/moco-v3/r-50-1000ep/r-50-1000ep.pth.tar>
- MoCo v3 (ViT-Base) [12]: <https://dl.fbaipublicfiles.com/moco-v3/vit-b-300ep/vit-b-300ep.pth.tar>
- SwAV [6]: [https://dl.fbaipublicfiles.com/deepcluster/swav\\_800ep\\_pretrain.pth.tar](https://dl.fbaipublicfiles.com/deepcluster/swav_800ep_pretrain.pth.tar)
- BYOL [21]: <https://drive.google.com/file/d/1-5-049vsro9YW9WTokSc8CoSrmjKfieB/view?usp=sharing>
- Barlow Twins [62]: <https://dl.fbaipublicfiles.com/barlowtwins/ljng/checkpoint.pth>

Barlow Twins has a projection head with an output dimension of 8192. We have to use the variant of PCD with asymmetric loss to distill knowledge from Barlow Twins due to limited memory.